Malaysian Journal of Civil Engineering 26(3):397-413 (2014)

CRACKING RESPONSE OF CONCRETE GRAVITY DAMS UNDER SEISMIC LOADING

Ali Zine[1]* & Abdelkrim Kadid[2]

[1] *Department of Hydraulics, University of Batna, Algeria*
[2]*Department of Civil Engineering, University of Batna, Algeria*
[1, 2]*Laboratoire de Recherche en Hydraulique Appliqué (LRHYA), University of Batna, Algeria*

*Corresponding Author: *zineali7@yahoo.fr*

Abstract: In this paper are presented the results obtained from a nonlinear seismic analysis of concrete gravity dams. Three dams with different heights will be studied under the effect of several earthquake ground motions. The fluid-structure interaction will be considered using the added mass concept of Westergraad is used to simulate the fluid-structure interaction with the foundation assumed to be rigid. The smeared cracking approach is used to model the initiation and propagation of cracks through the dams. The response of the dam is characterized by evaluating modal characteristics, displacements and crack patterns. The results obtained will allow having an insight into the expected behavior of concrete dams under future expected earthquakes and indicate that dynamic characteristics of a dam and the frequency content of the ground motions are a couple of the key parameters to consider when assessing the seismic safety of concrete gravity dams.

Keywords: *Gravity dams, concrete, dynamic analysis, fluid-structure interaction, smeared cracking model.*

1.0 Introduction

Concrete gravity dams can be considered as vital infrastructures and play an important role in the inland waterway transportation systems. Since many of them are built in high seismicity area and have been operating for a long period of time, their performance under strong ground motions is a subject of public concern and research attention. Despite the fact that the seismic response of such massive structures has been the subject of extensive studies over the past decades, there are still issues that have not been investigated and fully understood. Although linear response structures allow having an insight into the behavior of concrete gravity dams under earthquakes, it is evident that a rigorous estimate of the seismic performance of a dam can be assessed only by a nonlinear analysis. Due to the low tensile strength of concrete, concrete is likely to experience cracking which can be either minor of severe. In case of minor cracking, there is no substantial effect on the global stiffness of a dam. However for cases of

severe cracks, the dynamic behavior is totally different from that of a linear response and must recourse to a nonlinear analysis. Cracking can be caused by several factors such as construction, alkali-aggregate reactions, and loading. Cracking in concrete dam body can be considered as one of the major type of damage models to concrete gravity dams during strong earthquakes. In numerical analysis, the discrete and the smeared crack models are considered major tools to consider the initiation and propagation of cracks thorough the dam body. The discrete approach uses fracture mechanics concepts to model discrete cracking observed. On one hand, this approach is potentially attractive since it allows the accurate determination of the geometry of each crack. But on the other hand, is has the disadvantage of requiring remeshing of the domain as the crack surface changes which is complex and computationally expensive. The smeared cracking model uses continuum models. It consists of modifying the constitutive law governing the behavior of concrete.

The nonlinear dynamic behavior of concrete gravity dams has been the subject of many studies. Pal (1976) studied the seismic response of Koyna dam using a smeared crack model to model the initiation and growth of cracking. Mlakar (1987) studied the nonlinear seismic response of three different gravity dam sections. The dam sections with different heights were selected to be representative of the most common designs. A linear constitutive model in compression and tension, coupled with the smeared crack approach were adopted. The hydrodynamic effects were approximated using Westergaard's assumption through lumped masses distributed along the upstream face. The numerical results obtained indicated that the examples sections completely cracked across the width, with most of the cracking initiating at the upstream edge of the base and at the locations of abrupt slope change along the downstream face. El-Aidi and Hall (1989a, 1989b) used the smeared cracking model with a strength criterion for crack detection. They performed parametric studies to assess the effects of initial conditions induced by severe winter temperature and the effects of hydrodynamic and foundation interaction mechanism on the nonlinear seismic behavior of the dam. Vergas-loli and Fenves (1989) carried out a nonlinear seismic analysis of a gravity dam considering the tensile cracking of concrete and the interaction between the dam and the compressible water. The results obtained from this study indicate that concrete cracking is an important nonlinear phenomenon and extensive cracking due to strong earthquakes may affect the stability of the dams. Bhattacharjee and Leger (1995) used a rotating smeared crack finite element model based on energy conservation principle to predict the static fracture behavior of concrete gravity dam water penetration. Mao and Taylor (1997) studied the nonlinear dynamic response of concrete gravity dams. They indicated that the choice of a reliable concrete constitutive model and constitutive parameters to predict the performance of concrete gravity dams under earthquakes is a challenging task. The response of a typical medium height dam is examined suing ADINA package. Yamaguchi *et al*. (2004) indicated that rigorous evaluation of the performance of typical concrete gravity dam subjected to strong ground motions requires accurate modeling of the nonlinear characteristics associated with the tensile behavior of the mass concrete.

Thus nonlinear time history analysis is required to directly estimate the severity and extension of damage that could be expected. The results obtained showed that nonlinear procedures can identify the ultimate capacity of existing concrete gravity dam taking into account the most critical phenomena controlling the response and that the influence of input parameters and ground motions of the nonlinear dynamic response should be investigated by sensitivity analysis. Cai *et al*. (2008) developed a smeared crack model bases on nonlinear fracture mechanics. They then carried out a mesh objectivity verification study that showed that the proposed crack modeling method is mesh objective. A benchmark dam and an existing dam were analyzed numerically. Sensitivity study on the material fracture properties and fracture parameters was used to investigate the uncertainties often encountered in this type of analysis. Mansouri *et al*. (2011) have studied using the finite element method in the seismic fracture behavior of a concrete gravity dam. The Bazant model which is based on nonlinear fracture was used as a criterion to measure the growth of cracking and the smeared cracking model was chosen to develop crack profiles. The results obtained provide profiles of growth of expansion with and without the effects of reservoir.

2.0 Finite Elements Models

2.1 Structural Geometry

The structural geometries of the three concrete dams used in this study are shown in figure 1. The first dam is 36.30 m high with a base of 25.77 m. The second one is 60 m high with a base of 45.50 m. The last one has a height of 100 m with a base of 90 m.

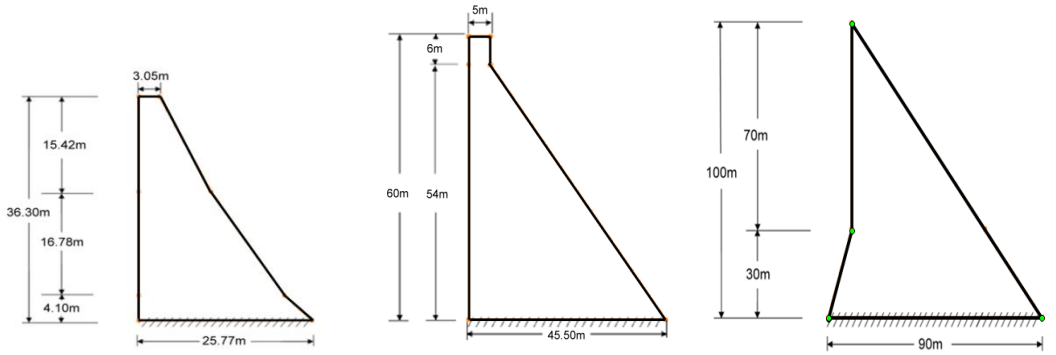

Figure 1: Geometry and dimensions of the dams

2.2 Finite Element Mesh

The models of dam A, B, and C consist of 280, 450, and 880 four nodded quadrilateral isoparametric plane strain elements respectively, see figure 2.

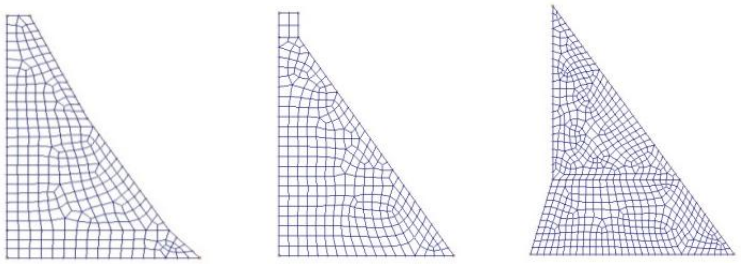

Figure 2: Finite element models of the dams

2.3 Material Modeling

It is well accepted that concrete is a very complex material. In this study, the concrete model implemented in ADINA (2013) has been adopted. Three features are necessary to realistically describe the material behavior:

- a stress-strain relation to include the high concrete nonlinearity.
- a failure surface that define tensile and compressive failure.
- a suitable technique to implement the post-cracking and crushing behavior.

In figure 3 is shown the compressive stress-strain relation for uniaxial and multiaxial stress conditions. Different curve parameters are considered depending on whether the material is in loading or unloading conditions.

The material assumed orthotropic with respect to the principal stress directions. If cracking occurs in any direction, that direction is fixed from that point onward in the computations. The Poisson ratio is assumed to be constant under tensile stresses and variable in the compressive region to allow capturing the dilatancy.

The failure envelopes, based on principal stresses, are shown in figures 4 and 5.

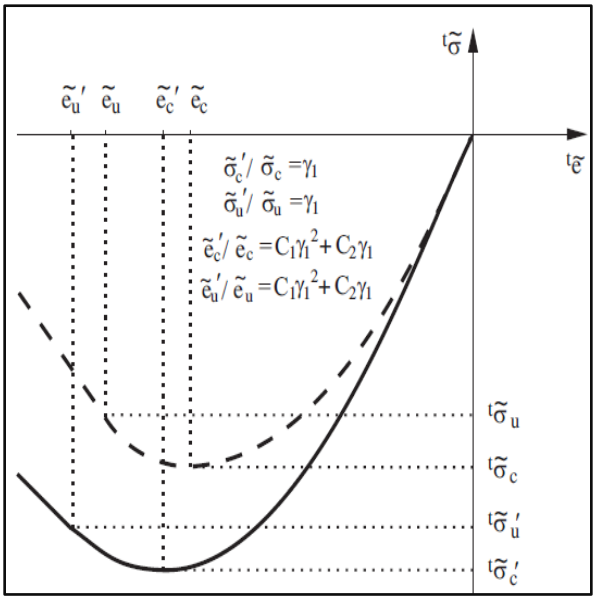

Figure 3: Compressive stress-strain behaviors

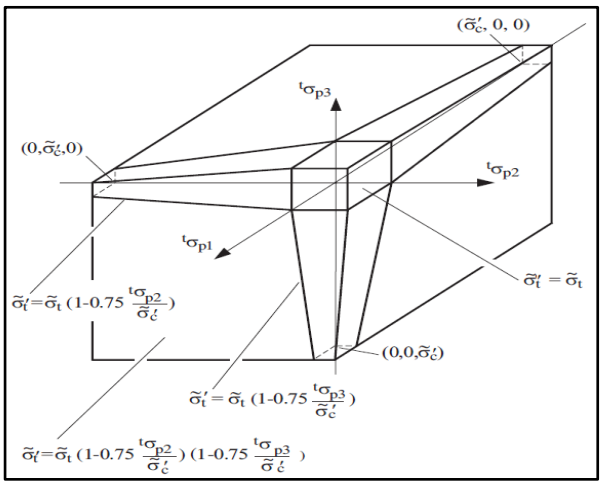

Figure 4: Tensile failure envelope

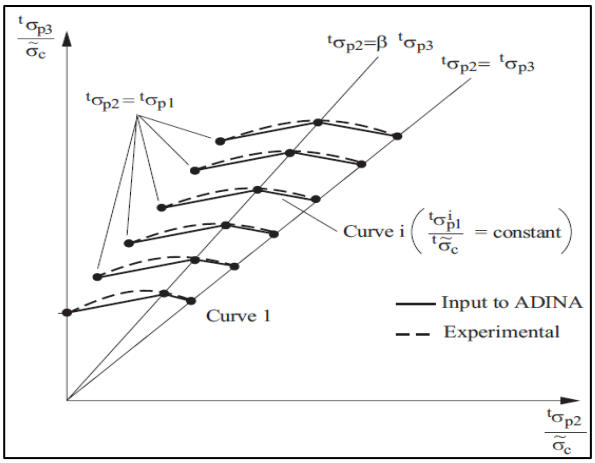

Figure 5: Triaxial compressive failure envelope

After cracking, it is assumed that a failure plane develops perpendicular to the corresponding principal stress direction. Thus, the normal and shear stresses across the failure plane are reduced and plane stress conditions are assumed. Thus, the normal and shear stiffness's across the failure plane are reduced and plane stress conditions are assumed. These stiffness's reductions are considered by using two constants following the shear retention factor concept. Typically, η_n= 0.0001and η_s= 0.5. The factor η_n is not exactly equal to zero in order to avoid the possibility of a singular stiffness. Figure 7 shows the material behavior in the direction normal to the tensile failure plane. ξ is a user defined variable which determines the amount of tension stiffening. To obtain a mesh independent solution, the fracture energy G_f can be directly provided and therefore, ξ is evaluated at each integration point based on the finite element size, figure 7.

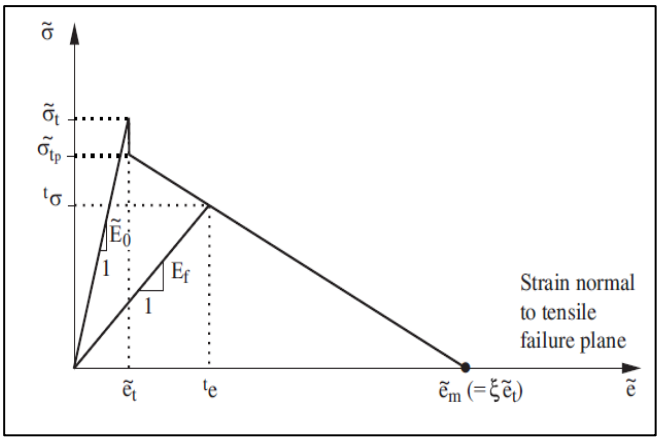

Figure 6: Uniaxial tensile behavior

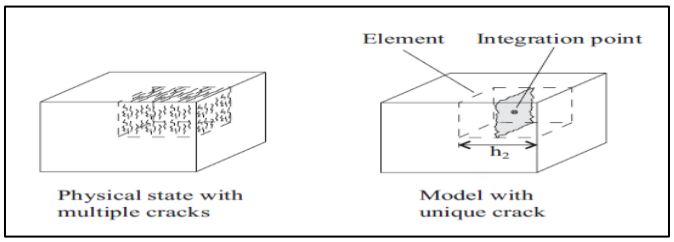

Figure 7: Parameter ξ calculation

$\xi=\frac{2\tilde{E}_0 G_f}{\tilde{\sigma}_t^2 h_2}$ *with* G_f *energy released per unit area in direction perpendicular to* h_2 *direction*

The shear module in the tensile failure plane also depends on the strain normal to that plane: The module is written with the parameter η_f which follows the law in figure 8. In each solution step, the crack is checked in order to verify whether the failure is still active. The failure is considered inactive in the normal strain across the plane becomes negative or less than the strain at which the last failure occurred; otherwise it is active.

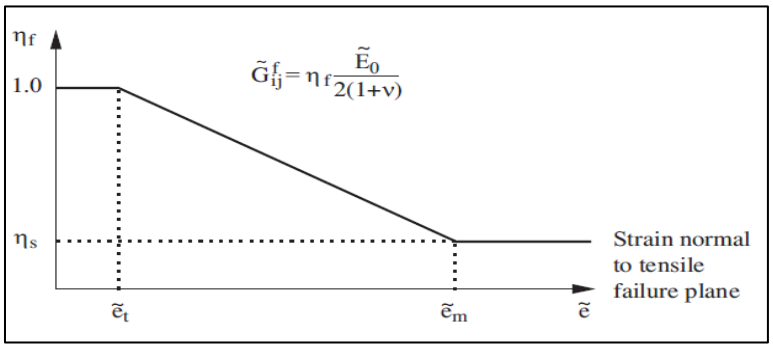

Figure 8: Parameter η_f calculation

The stress-strain relationship in the structure prior to cracking is expressed as:

$$\Delta = D\Delta \boldsymbol{\varepsilon} \quad (1)$$

Where, D is tangential material matrix and

$$\Delta\boldsymbol{\varepsilon} = \Delta\varepsilon^{co} + \Delta\varepsilon^{cr} \quad (2)$$

in which $\Delta\boldsymbol{\varepsilon}$ is the total strain increment,

$\Delta\varepsilon^{cr}$ is the strain increment of the crack,

$\Delta\varepsilon^{co}$ is the strain increment of the concrete between cracks and the stress increment for the plain strain problem.

$$\begin{Bmatrix}\Delta\sigma_{11}\\ \Delta\sigma_{22}\\ \Delta\sigma_{12}\end{Bmatrix} = \lambda\begin{bmatrix}1 & \frac{\nu}{1-\nu} & 0\\ \frac{\nu}{1-\nu} & 1 & 0\\ 0 & 0 & \frac{1-2\nu}{2(1-\nu)}\end{bmatrix}\begin{Bmatrix}\Delta\varepsilon_{11}\\ \Delta\varepsilon_{22}\\ \Delta\,\varepsilon_{12}\end{Bmatrix} \tag{3}$$

Where λ, ν and E are lama's constant, Poisson's and Young's module successively.

After the first cracking, the stress-strain relationship in the local axis is expressed as

$$\begin{Bmatrix}\Delta\sigma_{11}\\ \Delta\sigma_{22}\\ \Delta\sigma_{12}\end{Bmatrix} = \begin{bmatrix}0 & 0 & 0\\ 0 & \frac{E}{1-\nu^2} & 0\\ 0 & 0 & \beta G\end{bmatrix}\begin{Bmatrix}\Delta\varepsilon_{11}\\ \Delta\varepsilon_{22}\\ \Delta\,\varepsilon_{12}\end{Bmatrix} \tag{4}$$

Where G and β are shear modulus and shear retention factor respectively. After the development of the second crack in the direction perpendicular to the first, the stress strain relationship reduces to

$$\begin{Bmatrix}\Delta\sigma_{11}\\ \Delta\sigma_{22}\\ \Delta\sigma_{12}\end{Bmatrix} = \begin{bmatrix}0 & 0 & 0\\ 0 & 0 & 0\\ 0 & 0 & \beta G\end{bmatrix}\begin{Bmatrix}\Delta\varepsilon_{11}\\ \Delta\varepsilon_{22}\\ \Delta\,\varepsilon_{12}\end{Bmatrix} \tag{5}$$

The material properties adopted in this study are shown in table 1.

Table 1: Material properties

E_c(MPa)	N	$f_c^{'}$(MPa)	f_t(MPa)	G_f(N/mm)
32000	0.20	25000	25	200

Where E_c is the Young's modulus, ν is the Poisson's ratio, f_c' is the maximum uniaxial compressive strength, f_t is the maximum uniaxial tensile strength and G_f is the fracture energy.

2.4 Ground Motions

Four earthquake records have been used in this study, figure 9. The Dar El Beidha accelerogram recorded during the Boumerdes (Algeria) earthquake of 2003, The Chichi accelerogram recorded during the Taiwan earthquake of 1999, The Sakara accelerogram recorded during The Kocaeli (Turkey) earthquake of 1999 and the Corralitos accelerogram recorded during the USA earthquake of 1989. The characteristics of the records are shown in table 2.

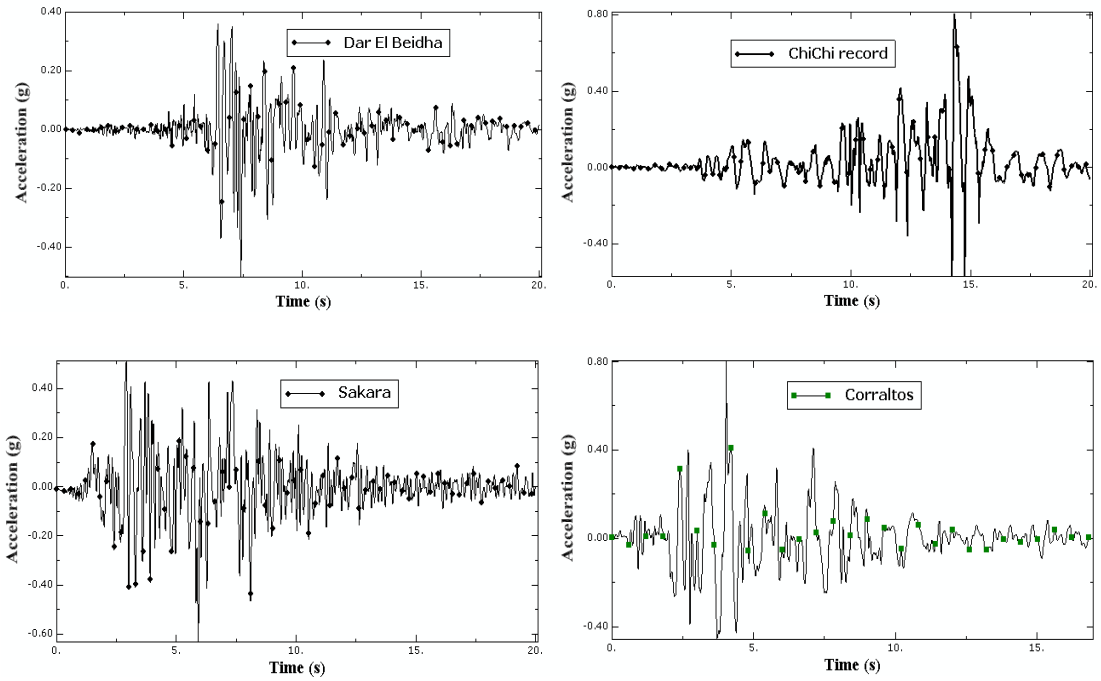

Figure 9: Earthquake records used

Table 2: Ground motion characteristics

Record	*Maximum Acceleration*	*Maximum Velocity*	*Arias Intensity*	*Specific Energy Density*	*Acceleration Spectrum Intensity*	*Velocity Spectrum Intensity*	*Effective Design Acceleration (EDA)*
Chichi	0.808g at time t=14.3 s	680.434 cm/s at time t=15.980s	5.191m/s	2582171.055cm^2/s	0.654g*s	261.992 cm	0.835g
Corralitos	0.799g at time t=4.040s	58.814 cm/s at time t=3.960s	4.218m/s	3952.893 cm^2/s	0.448g*s	246.713 cm	0.636g
Dar-El-Beidha	0.499g at time t=7.410s	39.865 cm/s at time t=7.070s	1.875m/s	2326.135 cm^2/s	0.442g*s	131.025 cm	0.487g
Sakara	0.628g at time t=5.920s	77.369 cm/s at time t=6.320s	4.753m/s	7127.971 cm^2/s	0.548g*s	266.838 cm	0.534g

3.0 Nonlinear Dynamic Analysis

Prior to the application of the dynamic loading, static loading was considered. In transient dynamic analysis, the following system of dynamic equilibrium equations is solved at each time t:

$$[M]\{\ddot{u}(t)\} + [C]\{\dot{u}(t)\} + \left(f_{int}(\{u\},\{\dot{u}\},\{\varepsilon\},\{\sigma\},t,\dots\dots)\right) = \{f_{ext}(t)\} \qquad (6)$$

Where $[M]$ and $[C]$ are the mass and damping matrices respectively, and $\{f_{ext}(t)\}$ is the vector of external forcing functions. The vectors$\{\ddot{u}(t)\}$,$\{\dot{u}(t)\}$, and $\{u(t)\}$ are the resulting accelerations velocities and displacements, respectively. The vector$\{f_{int}(t)\}$ is the internal set of forces opposing the displacements and is usually dependent on the displacements, velocities, and field of strains$\{\varepsilon\}$ and stresses $\{\sigma\}$.In this study, a Rayleigh type damping is adopted. It is based on a linear combination of the mass matrix$[M]$ and the linear elastic stiffness matrix or the tangent stiffness $[K]$ as follows:

$$\alpha[M] + \beta[K] \qquad (7)$$

Where the coefficients α and β are determined to provide for two selected damping ratios for two specific modes of vibration, in the first two modes.

The direct integration of the above equations is required. One of the most widely used methods is the Newmark method with automatic time stepping. For large number of degrees of freedom, the numerical damping feature is essential to suppress undesirable higher modes.

The hydrostatic load was applied as pressure loading on the upstream face of the dam. The hydrodynamic loading of the reservoir was approximated by the Westergraad method of added masses. Due to the fact that strength based criterion for crack analysis of concrete structures can cause the results to be mesh sensitive, that is stresses become progressively larger as the mesh around the crack tip is refined, the fracture mechanics approach bases on energy principles has been adopted in this study, this is a rational technique for analyzing the initiation and the growth of cracks in concrete structures.

4.0 Results and Discussion

4.1 Modal Results

The periods of the three dams are shown in table 3.

Table 3: Periods of the structures in seconds

Structures	*Mode 1*	*Mode 2*	*Mode 3*
Dam A	0.1307	0.04983	0.04021
Dam B	0.1939	0.08312	0.06526
Dam C	0.2847	0.1293	0.1016

4.2 Cracking Profiles

The cracks patterns in dam A under the different earthquake records are shown in figure 10. For all the earthquake records, most of the cracking is concentrated on the downstream face with a tendency to propagate towards the body of the dam. However, the initiation of cracking at the base is largely dependent on the ground motion record used. For this dam, the level of damage is relatively small.

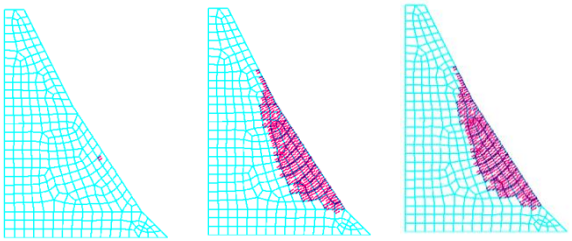

Dar El Beidha record

t = 8.50 s t = 12.00 s t = 16.00 s

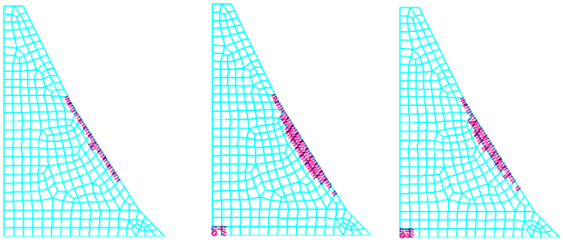

Corralitos record

t =4.44 s t =5.50 s t =10.20 s

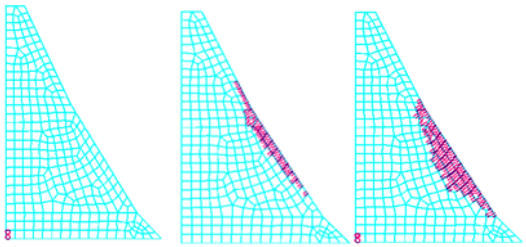

Sakara record

t = 6.10 s t = 6.43 s t =6.70 s

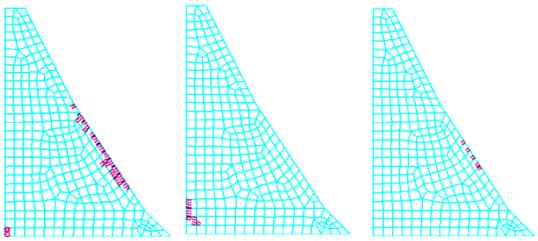

Chichi record

t = 15.94 s t =6.08 s t = 16.00 s

Figure 10: Crack profiles for dam A

For dam B, cracking is more important than that of dam A, figure 11. The upstream face can be cracked from the top to the base for the Chichi and Sakara records while for Dar El Beidha and Corralitos records there are less cracks on the upstream face and near the base. Again, the downstream face exhibits considerable cracking extending to the neck at the location of slope change.

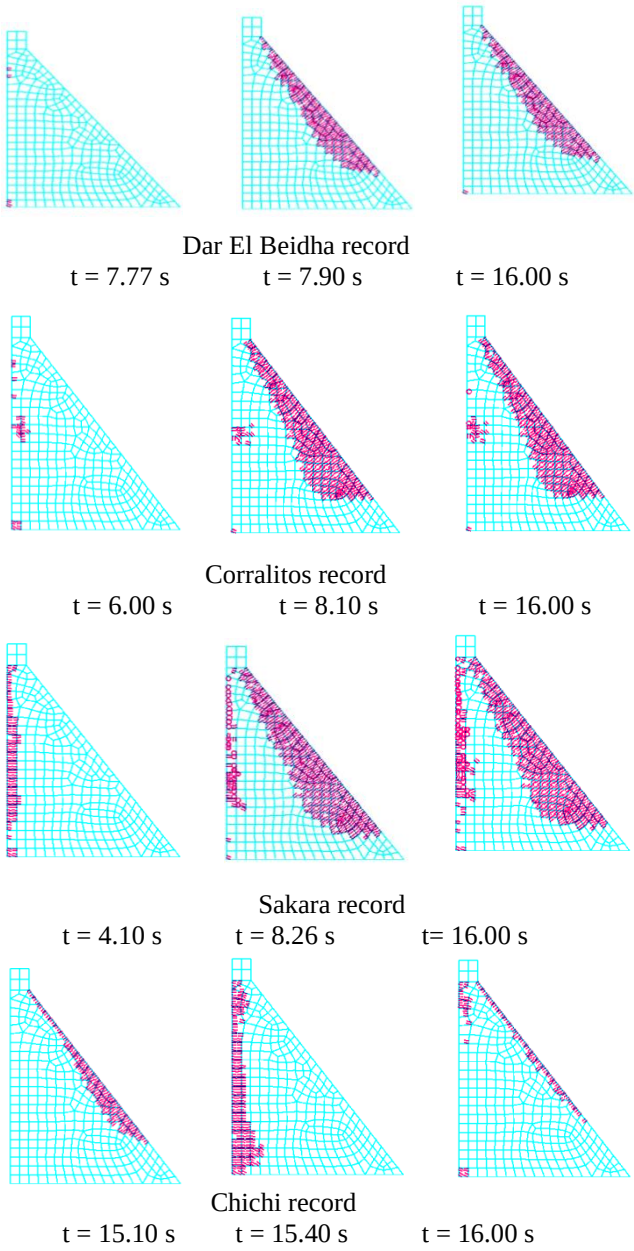

Figure 11: Crack profiles for dam B

In dam C, figure 12, the cracks occurred on the downstream face, at the base and at the location of slope change near the upstream face. For the Sakara and Corralitos records the analysis terminated prematurely. The cracks on the downstream face coalesced with those of the upstream face for the Dar El Beidha record for a time of 16 s. The influence of the frequency content of the ground motions is evident as the crack patterns differ for each record. The density of cracking is greater than that of dam A suggesting an influence of the dynamic characteristics of the dams.

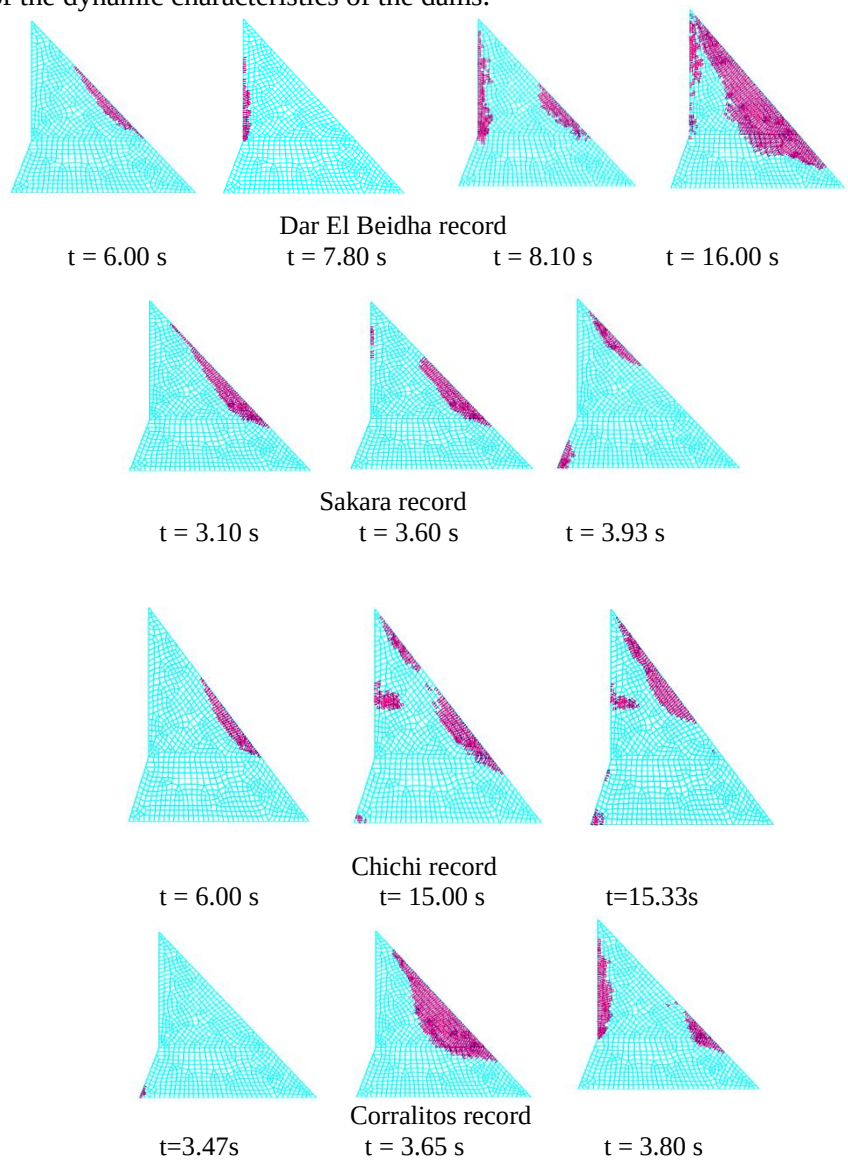

Figure12: Crack profiles for dam C

4.3 Displacements

According to Mao and Taylor (1997), if the cracking is near horizontal, the vertical displacement time history of a node can be taken as the crack mouth opening displacement. The node on the mid downstream face has been selected since for all dams and under all ground motions, most of cracking occurred in this zone. The selected nodes for the three dams are: 56, 45 and 105 as shown in figure 13.

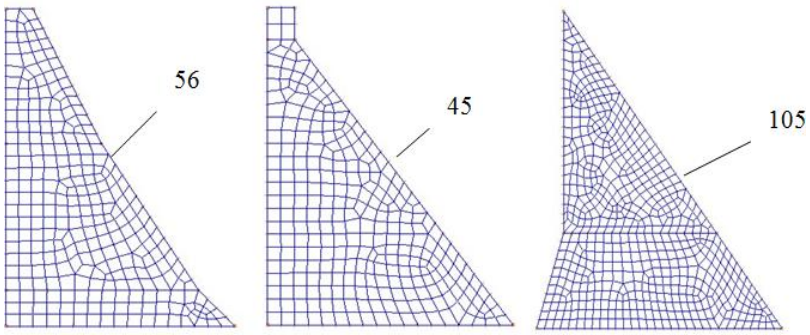

Figure 13: The selected node

The maximum vertical displacements for dam A are 0.79 mm, 0.668 mm, 0.781 mm and 0.775 mm for the Chichi, Corralitos, Dar El Beidha and Sakara records respectively. For Dam B and C, the values are 2.9 mm, 1.34 mm and 1.41 mm, and 1.58 mm, and 5.62 mm, 4.03 mm, 5.66 mm, and 1.64 mm respectively, see figure 14. Thus, the crack mouth opening displacement is more important for the dam with greater height.

5.0 Conclusions

The numerical analyses showed that cracking occurred mainly of the downstream face, at the base and the slope change near the upstream face. The dynamic characteristics of a dam are an important parameter that should be given attention in the seismic assessment of cracking in dams since they influence the spread of damaged zones and the crack mouth opening which were found to be more important for flexible dams. The frequency content of earthquakes can change drastically the patterns of cracks. The downstream cracks tend to propagate through the body of the dam and to coalesce with those of the upstream face near the neck for dams B and C. The density of cracking for dam A is less important compared to that of dams B and C. The dynamic characteristics of a dam influence the crack mouth opening displacement which is more critical for flexible dams. And it is also noted that the hydrodynamic pressure is more significant to the response of the dam when the mass is distributed along the highest dam, where it tends to modify the global seismic response of the dam.

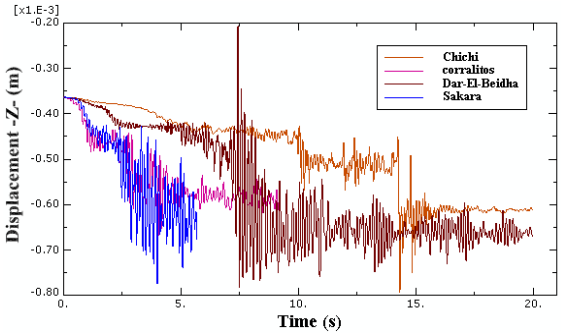

Dam A

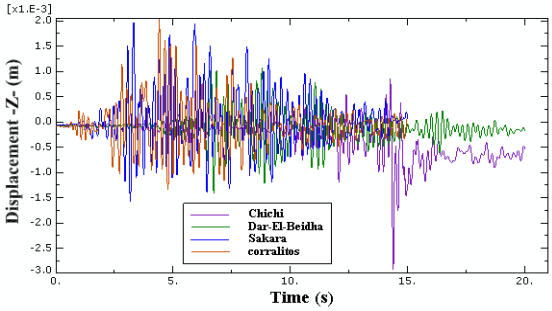

Dam B

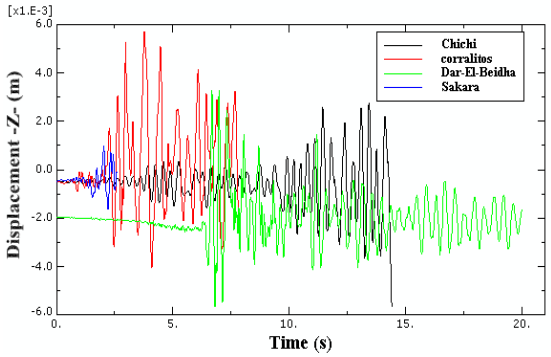

Dam C

Figure 14: Vertical displacements

References

ADINA, (2013). *Version 8.2, Users Manuals. ADINA; R& D, Inc., Watertown, Massachusetts, USA.*

Bhattacharjee, S.S., and Leger, P. (1995). *Fracture response of gravity dams due to rise of reservoir elevation.* Journal of Structural Engineering. September 1995. 1299-1305.

Cai, Q., Robberts, J.M., And Ransburg, B.W.J. (2008). *Finite element fracture modeling of concrete gravity dams.* Journal of the South African Institution of Civil Engineering, 50:1, 13-24.

El-Aidi, B., and Hall, J.F. (1989a). *Non-linear earthquake response of concrete gravity dams, Part 1: Modeling,* Earthquake Engineering and Structural Dynamics. 18, 837-851.

El-Aidi, B., and Hall, J.F. (1989b). *Non-linear earthquake response of concrete gravity dams, Part II: Behavior,* Earthquake Engineering and Structural Dynamics. 18, 853-865.

Mansouri, A., Neshaei, M.A.L., and Aghajany. R. (2011). *Fracture analysis of concrete gravity dam under earthquake induced loads.* Journal of Applied Sciences, Environment, and Management.15 (2) 317-325

Mao, M. and Taylor, C.A. (1997). *Nonlinear seismic cracking analysis of medium-height concrete gravity dams.* Computers and Structures. 64:5/6, 1197-1204.

Mlakar, P. (1987). *Nonlinear response of concrete gravity dams to strong earthquake-induced ground motions.* Computers and Structures. 26:1,165-173.

Pal, N. (1976). *Seismic cracking of concrete gravity dams.* Journal of the Structural Division (ASCE). 102:9, 1827-1844.

Vergas-loli, M. And Fenves, G.L. (1989). *Effects of concrete cracking on the earthquake response of gravity dams.* Earthquake Engineering and Structural Dynamics. 18, 575-592.

Yamaguchi, Y., Hall, R., Sasaki, T., Matheu, E., Kanenawa, K., Chudgar, A., and Yule. D. (2004). *Seismic performance evaluation of concrete gravity dams.* Proceedings of the 13th World Conference on Earthquake Engineering –Vancouver, Canada.